

# A Fluorescence-Based Assay System for the Determination of Haloperoxidase-Activity Using a Two-Dimensional Calibration Approach

Alexander V. Fejzagić,<sup>[a]</sup> Sebastian Myllek,<sup>[b]</sup> Fabian Hogenkamp,<sup>[b]</sup> Julian Greb,<sup>[b]</sup> Jörg Pietruszka,<sup>[b]</sup> and Thomas Classen<sup>\*[a]</sup>

Screening for an interesting biocatalyst and its subsequent kinetic characterization depends on a reliable activity assay. In this work, a fluorometric assay based on the halogenation of 4-methyl-7-diethylamino-coumarin was established to monitor haloperoxidase-activity. Since haloperoxidases utilize hydrogen peroxide and halide ions to halogenate a broad range of substrates by releasing hypohalous acids, a direct quantification of haloperoxidase-activity remains difficult. With the system presented here, 3-bromo-4-methyl-7-diethylaminocoumarin is preferentially formed and monitored by fluorescence measure-

ments. As starting material and product share similar spectroscopical properties, a two-dimensional calibration approach was utilized to allow for quantification of each compound within a single measurement. To validate the system, the two-dimensional Michaelis-Menten kinetics of a vanadium-dependent chloroperoxidase from *Curvularia inaequalis* were recorded, yielding the first overall kinetic parameters for this enzyme. With limits of detection and quantification in the low  $\mu\text{M}$  range, this assay may provide a reliable alternative system for the quantification of haloperoxidase-activity.

## 1. Introduction

Halogenated compounds may have severely different (bio-)chemical and (bio-)physical properties compared to their non-halogenated analogues. One of the most prominent examples is vancomycin, where its chlorine substituents define the rigidity of the juxtaposed aromatic rings and thereby dictate the molecules overall stability and specificity regarding the binding site to peptides.<sup>[1]</sup> Other examples show the increased biological activity of brominated aminophenols against different microorganisms.<sup>[2]</sup> These changes in intermolecular interaction can be employed for the synthesis of pharmaceutical drugs or as precursors for the synthesis of commonly used building blocks.<sup>[3]</sup> Chemical halogenation requires the use of elemental halogens or agents derived from them, like *N*-chlorine/bromine succinimide, thionyl chloride, trimethylsilyl iodide, bearing problems of high energy demand during production and severe toxicity. In contrast, halogenating

enzymes are capable of introducing halogens to electron-rich substrates using halides.<sup>[4]</sup>

A screening for biocatalytically interesting haloperoxidases (HPOs) and a proper kinetic description depends on a reliable activity assay. Haloperoxidases generate hypohalous acid from the respective halides ( $\text{Cl}^-$ ,  $\text{Br}^-$ ) and hydrogen peroxide, releasing this electrophilic halogen species from the active site so that the subsequent halogenation of a substrate does not necessarily have to take place within the active site (see Scheme 1A). The most common assay for quantifying haloperoxidase-activity is the dimedone (**1**) assay, where the amount of mono-halodimedone **2** is photometrically measured at 290 nm (see Scheme 1.B).<sup>[5]</sup> The highly nucleophilic dimedone (**1**) can be halogenated to mono-halodimedone **2** and consecutively to dihalodimedone **3**. In order to have a one-to-one-conversion readout mono-halodimedone **2** is used as an assay substrate – a compound which is commercially hardly available or very expensive as mono-chlorodimedone ( $\text{X}=\text{Cl}$ ) and is virtually not available in the case of mono-bromodimedone ( $\text{X}=\text{Br}$ ).

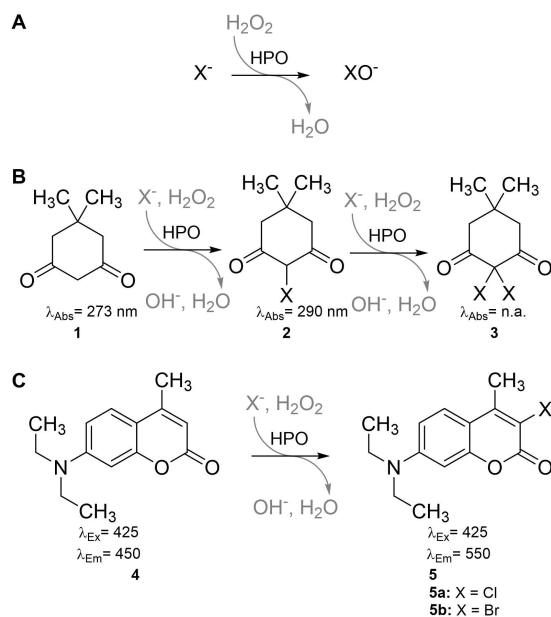
Furthermore, the assay is compromised by other reasons: the absorption of compound **2** superimposes with the absorption of aromatic proteinogenic amino acids, which may be tolerable because of the low and constant concentration of proteins within the assay. More severely, due to several possible decomposition reactions of both compounds, **2** and **3**, the readout of this assay can lead to false-positive hits in enzymatic screening.<sup>[6]</sup> Applying correction factors, this error can be mathematically smoothed, nevertheless, the measurement remains flawed. The absorption spectra of dimedone and mono-chlorodimedone show a high overlap and therefore raise the question how precisely activity can be measured if dimedone is in a high excess at the start of the reaction (see SI figure 14). Other assay systems are usually focused on the

[a] A. V. Fejzagić, Dr. T. Classen  
Institute for Bio- and Geosciences I: Bioorganic Chemistry  
Forschungszentrum Jülich GmbH  
D-52426 Jülich (Germany)  
E-mail: t.classen@fz-juelich.de

[b] S. Myllek, F. Hogenkamp, J. Greb, Prof. Dr. J. Pietruszka  
Institut für Bioorganische Chemie  
Heinrich-Heine-Universität Düsseldorf im Forschungszentrum Jülich  
D-52426 Jülich (Germany)

Supporting information for this article is available on the WWW under <https://doi.org/10.1002/open.202000184>

© 2020 The Authors. Published by Wiley-VCH GmbH. This is an open access article under the terms of the Creative Commons Attribution Non-Commercial License, which permits use, distribution and reproduction in any medium, provided the original work is properly cited and is not used for commercial purposes.



**Scheme 1.** a) The haloperoxidase (HPO) forms hypohalites ( $\text{OX}^-$ ) from hydrogen peroxide and halides ( $\text{X}^-$ ). b/c): General reaction scheme for (B) the dimedone (1) assay and (C) the fluorescence assay presented in this work. The halogenation causes a change in the absorption spectrum of either dimedone (1) or the fluorescence properties of 4-methyl-7-diethylamino-coumarin (MeDAC, 4).

detection of hypohalide species and therefore may be adapted for the determination of haloperoxidase activity. The taurine chloramine assay utilizes 3,3',5,5'-tetramethylbenzidine in a coupled reaction to make the chlorination of taurine visible at 650 nm. Another system is based on *p*-cresol, a fluorescent probe which is sensitive to halogenation as all halogenated derivatives lose their fluorescence properties and therefore allow monitoring the reaction via *p*-cresol depletion. Other examples include fluorescein derivatives, which are oxidized after halogenation to fluorescein, one of the most prominent fluorescent probes used in molecular medicine. The main problem for an adaption of these assays as a HPO assay is the oxidative environment of the assay. Besides the hypohalous acid, hydrogen peroxide, as a very strong oxidant which is capable to oxidize most of the mentioned compounds, is required in the solution as well. For 3,3',5,5'-tetramethylbenzidine, for instance, it is a known fact that hydrogen peroxide may oxidize the compound itself, flawing the measurement. If a qualitative answer is sufficient, the phenol red assay is sensitive for HPO activity by halogenating phenol red four times to yield bromophenol blue. Again, no enzyme kinetic data can be acquired using this system.

Comparing kinetic values determined for some HPOs show remarkable differences reported in literature (see Table 1).<sup>[7]</sup> As these enzymes catalyze a two-substrate enzymatic reaction, the relation between the kinetic parameters and concentration of both substrates has to be taken into account. Kinetics fixing the concentration of one reactant during its record yield only apparent kinetic parameters ( $K_M$ ,  $v_{\max}$ ). A direct comparison of two datasets bearing apparent values only is hardly possible.

**Table 1.** Kinetic parameters of  $V_G$ PO from *C. inaequalis* determined with the MeDAC-assay at pH 6 compared to previously published parameters using the MCD-assay.

kinetic data	MeDAC-assay this work	MCD-assay data from ref. <sup>[5b]</sup>	MCD-assay data from ref. <sup>[7b]</sup>
$K_M(\text{Br}^-)$	$0.19 \pm 0.04$ [mM]	$0.12^a$ [mM] $0.007$ [mM]	$0.026$ [mM]
$K_M(\text{H}_2\text{O}_2)$	$1.48 \pm 0.23$ [mM]	$< 0.005^a$ [mM]	$0.003$ [mM]
$K_i(\text{Br}^-)$	$56.80 \pm 6.97$ [mM]	n.a.	n.a.
$K_i(\text{H}_2\text{O}_2)$	n.a.	n.a.	n.a.
effective	$9.80 \pm 0.73$ [ $\text{s}^{-1}$ ]	n.a.	n.a.
$k_{\text{cat}}$			
apparent	$7.0 \pm 8.9^b$ [ $\text{s}^{-1}$ ]	$100$ ( $\text{Br}^-$ ) [ $\text{s}^{-1}$ ] <sup>d</sup>	$21.3$ ( $\text{Br}^-$ ) [ $\text{s}^{-1}$ ]
$k_{\text{cat}}'$	$8.5 \pm 0.8^c$ [ $\text{s}^{-1}$ ]	$37$ ( $\text{Br}^-$ ) [ $\text{s}^{-1}$ ] <sup>d</sup> $33$ ( $\text{H}_2\text{O}_2$ ) [ $\text{s}^{-1}$ ]	$15.2$ ( $\text{H}_2\text{O}_2$ ) [ $\text{s}^{-1}$ ]

[a] The reported  $K_M$  values were determined at pH 8. [b/c] The value for  $k_{\text{cat}}$  was calculated using the obtained fit function (see SI '2D-kinetics') and inserting the concentrations of [b]  $\text{Br}^-$  (10 mM) and [c]  $\text{H}_2\text{O}_2$  (10 mM) used in previous works to allow for a better comparison<sup>[7b]</sup>. The error was calculated using standard error propagation rules. [d] Multiple  $k_{\text{cat}}$ -values were given in Wever, et al.<sup>[5b]</sup>

Additionally, these partial data sets do not necessarily allow the evaluation of the overall performance of the enzyme for biocatalytic approaches. Therefore, we aimed at providing an alternative system for reproducible results based on readily available substrates to obtain a general kinetic data set for HPOs. The fluorescent sensor 4-methyl-7-diethylamino-coumarin (MeDAC 4, see Scheme 1.C) which offers an activated position for electrophilic aromatic substitution reactions was chosen. This compound was already investigated as a sensor for medically relevant hypohalous acid formation observed in inflammation reactions and characterized as a very reliable and sensitive hypohalous acid sensor, *in vitro* and *in vivo*.<sup>[8]</sup> Using this sensor, a time-resolved quantification assay for hypobromite using a mixed fluorescence readout was established. This ultimately allowed the record of a complete set of absolute rather than apparent kinetic data on a HPO.

## 2. Results and Discussion

### 2.1. Approach

MeDAC was used as a fluorescence reporter because it conducts the halogenation to one specific position due to the high nucleophilicity, which is the 3-position juxtaposed to the carbonyl carbon of the lactone moiety. MeDAC, as a coumarin-derivative, is a potent fluorophore, and its halogenated derivatives have already been tested for fluorescence as well.<sup>[9]</sup> Thus, a fluorophore promises high sensitivity, which is generally favored for enzymatic samples with potential small concentrations of compound and enzyme required. Additionally, it should be possible to use this fluorescence probe for measuring the depletion rate of starting material and formation rate of product simultaneously. Since the common hypothesis is that halogenation does not occur at the active site of the enzyme, the rate-limiting step is assumed to be the formation of the highly reactive halogenating species (e.g. HO-X) and not the

halogenation of the target compound itself.<sup>[10]</sup> During our studies on the development of the assay, it was shown early on that both MeDAC and the mono-brominated compound BrMeDAC are subject to quenching in fluorescence and that the components are also capable of quenching each other. This makes the simultaneous measurement of both components necessary. In the following, we describe how the assay was developed and evaluated (see Figure 1). To guide the reader through the procedure, circled numbers have been added to each step to visualize the experiments and rationale behind the assay development (see Figure 1 A). If the system is adapted,

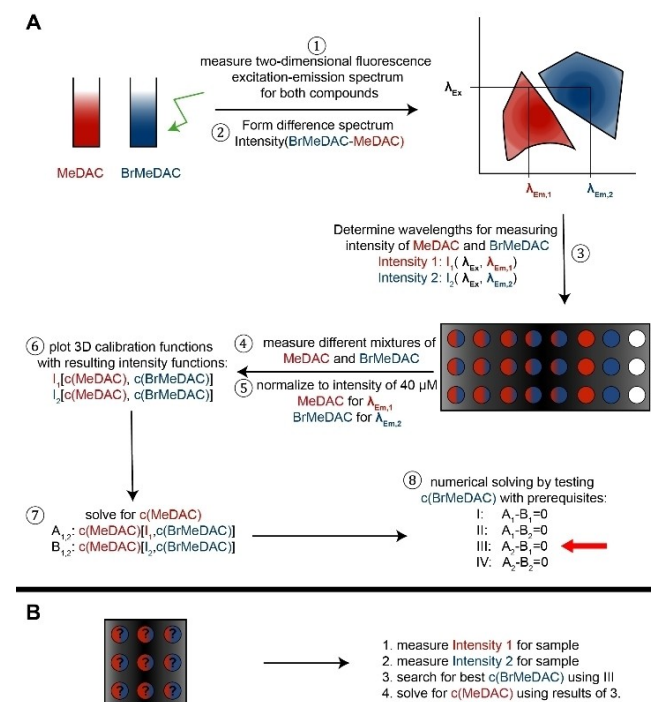


**Figure 1.** Workflow for the creation, calibration (A) of the MeDAC-assay and measurement of haloperoxidase-activity (B)

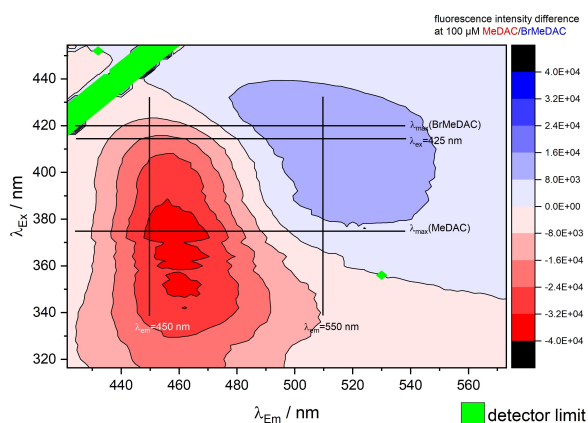


**Figure 2.** Projection of the difference-fluorescence spectrum values ( $\text{fluorescence} - \text{difference} = \frac{I(\lambda_{Ex}, \lambda_{Em})_{\text{BrMeDAC}}}{c_{\text{BrMeDAC}}} - \frac{I(\lambda_{Ex}, \lambda_{Em})_{\text{MeDAC}}}{c_{\text{MeDAC}}}$ ) in 100 mM Bis-TRIS (pH 6), 1% (v/v) DMSO and 100  $\mu$ M of fluorophore. Green encodes for values exceeding the detector limit, blue encodes for net-fluorescence of BrMeDAC (5b) and red for net-fluorescence of MeDAC (4).

the required steps to acquire HPO activity are summarized as well (see Figure 1 B). As an application example, the performance of the assay is shown on multi-dimensional steady-state kinetics for the haloperoxidase  $V_{Cl}PO$  from *Curvularia inaequalis*.

## 2.2. Fluorescence Properties and Assay Parameters:

While MeDAC (4) is commercially available, the reference compound BrMeDAC (5b) was synthesized following an established protocol.<sup>[9]</sup> For both, MeDAC and BrMeDAC (5b), concentration-normalized 2D-fluorescence spectra in 100 mM Bis-TRIS buffer have been measured (see Figure 1a ①), from which a difference spectrum was calculated in order to identify a combination of one single excitation wavelength ( $\lambda_{Ex}$ ) and two emission wavelengths ( $\lambda_{Em}$ ) with high intensity for both fluorophores ② (see Figure 2). An equation with two variables [ $c(\text{MeDAC})$ ,  $c(\text{BrMeDAC})$ ] must be solved as both compounds exhibit fluorescence and therefore influence the correlation between fluorescence intensity and concentration of each compound. This can be achieved by two independent intensity measurements. Using only one excitation wavelength is advantageous for kinetic measurements because the technical time in between two measuring events can be reduced and the calibration can be simplified. The phosphate-free buffer was chosen because the subsequent experiments were performed with a vanadium-dependent HPO from *C. inaequalis*, which is inhibited by phosphate.<sup>[5b]</sup> It should be highlighted here that the fluorophores are dependent on the buffer system used, which makes an individual calibration necessary [corresponding spectra and calibration in 100 mM  $KP_i$ -buffer (pH 3) can be found in the SI].

In a first step, a two-dimensional fluorescence excitation-emission-spectrum was measured with 100  $\mu$ M of MeDAC and BrMeDAC. Forming the difference of the fluorescence intensity of MeDAC from BrMeDAC at the given excitation and emission wavelengths ( $\lambda_{Em}$  and  $\lambda_{Ex}$ ) yields the difference-fluorescence spectrum (eq. 1, see Figure 2):

$$\text{fluorescence} - \text{difference} = \frac{I(\lambda_{Ex}, \lambda_{Em})_{\text{BrMeDAC}}}{c_{\text{BrMeDAC}}} - \frac{I(\lambda_{Ex}, \lambda_{Em})_{\text{MeDAC}}}{c_{\text{MeDAC}}} \quad (1)$$

From the difference spectrum (see Figure 2) the following measuring parameters have been derived for 100 mM Bis-TRIS (pH 6) with 100 mM fluorophore, 1% (v/v) DMSO (③), ensuring an at least 3-fold higher fluorescence intensity of the investigated compound at the given emission wavelength compared to the other fluorophore (i.e. MeDAC emission is three-fold higher at 450 nm emission wavelength than BrMeDAC and *vice versa* at 550 nm emission, eq. 2 and 3).

$$\lambda_{Ex}^{\text{all}} = 425 \text{ nm}; \lambda_{Em}^{\text{MeDAC}} = 450 \text{ nm} \quad (2)$$

$$\lambda_{Em}^{\text{BrMeDAC}} = 550 \text{ nm} \quad (3)$$

In an ideal case for the calibration, the individual fluorescence intensity values for both fluorophores would simply sum-up to the actual intensity, while each intensity would scale linearly and independently of the other fluorophore with its concentration. Such plane equations could be solved analytically with two independent measurements. However, there are fluorescence-quenching and inner filter effects for the pure samples as well as mixtures of MeDAC and BrMeDAC. To take all of these effects into account, the measured total intensity at each emission wavelength was plotted against the concentration of MeDAC and BrMeDAC in the sample, leading to complex surfaces. The complex surfaces can be fitted by a 2<sup>nd</sup> order polynomial surface function for both emission wavelengths when measuring MeDAC and BrMeDAC separately – as well as in reasonable mixtures (④, see Figure 3). Due to the low solubility of BrMeDAC in aqueous solutions, the highest concentration was set to 100  $\mu\text{M}$ . The obtained data points were then fitted using a 'Poly2D'-fit in OriginPro 2018. In contrast to the KP<sub>1</sub>-buffer (see SI Figures 5 & 6), the pH-shift in Bis-TRIS buffer at pH 6 led to a quenching of BrMeDAC at about 40–50  $\mu\text{M}$  visible through the decrease in the slope. Therefore,

the maximum concentration calculable in this buffer system for BrMeDAC is assumed to 40  $\mu\text{M}$ . Technically, the fluorescence intensity depends on the excitation intensity, detector sensitivity and integration times applied by the fluorimeter. To circumvent tedious calibrations with each measuring campaign the fluorescence intensities were normalized to the intensity at  $c(\text{MeDAC}) = c(\text{BrMeDAC}) = 40 \mu\text{M}$  measured at the emission wavelengths of MeDAC (450 nm) and BrMeDAC (550 nm), respectively(⑤) (see SI Figures 7 & 8 for final calibration used).

The polynomial surface functions (⑥) obtained by the calibration and fit were mathematically resolved to  $c(\text{MeDAC})$ . This yields four equations (⑦), which still contain the second variable  $c(\text{BrMeDAC})$ . These equations could not be further solved analytically. However, it is also true that two of these equations will always have the same value for a certain concentration of MeDAC in the measuring range, respectively the difference will be 0. This condition was used to finally solve the system of equations numerically (⑧) (see SI). For this purpose, the solver was used in Microsoft Excel, which can also be used as a macro automated solver for large tables of measured values such as kinetics.

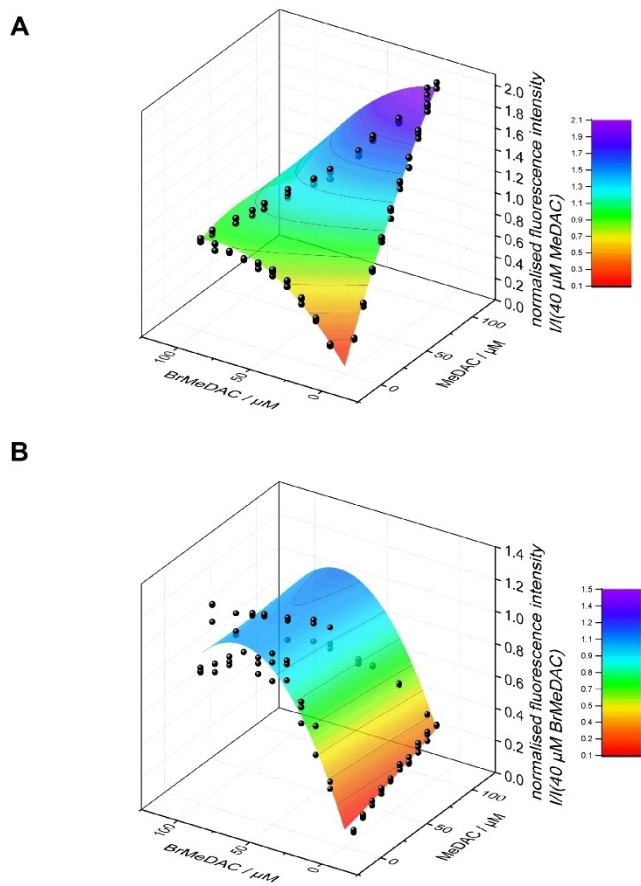


**Figure 3.** a) Fluorescence intensities in dependence of concentrations of MeDAC and BrMeDAC in 100 mM Bis-TRIS (pH 6), normalized to the fluorescence of 40  $\mu\text{M}$  MeDAC or BrMeDAC, respectively [ $\lambda_{\text{Ex}}^{\text{all}} = 425 \text{ nm}$ ;  $\lambda_{\text{Em}}^{\text{MeDAC}} = 450 \text{ nm}$ ]. The values have been modelled using least-square fitting (software: OriginPro 2018) with a 2<sup>nd</sup> order 2D-polynomial ( $R^2 = 0.99$ ). b) Measurements of the very same samples at  $\lambda_{\text{Ex}}^{\text{all}} = 425 \text{ nm}$ ;  $\lambda_{\text{Em}}^{\text{BrMeDAC}} = 550 \text{ nm}$ ,  $R^2 = 0.96$ .

### 2.3. Proof of Principle and Evaluation

To validate the approach, different mixtures of MeDAC and BrMeDAC, which were not part of the calibration and sum up to a total concentration of 40  $\mu\text{M}$  in each sample, were tested and the calculated concentrations plotted against the actual ones (see Figure 4).

For an ideal correlation, the slope of the straight line should be 1 with no axis intercept and a  $R^2$  of 1. As shown in Figure 4, although the  $R^2$  shows a convincing precision, the slopes differ from that value, especially for BrMeDAC. The data of these plots have been used for introducing a correction term based on the

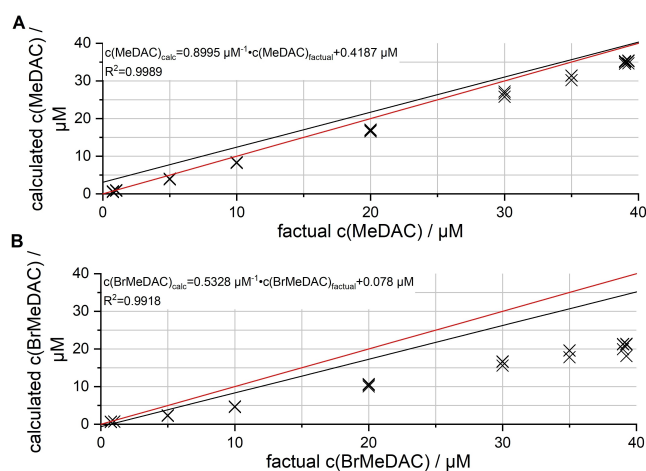


**Figure 4.** Calculated versus factual concentrations of MeDAC (A) and BrMeDAC (B). The red line represents the ideal case, in which the correlation between calculated and factual concentrations is perfect (slope = 1), the black line represents the measured and calculated concentrations in dependence of the factual ones.

equations for both lines, which increased the accuracy (see Figure 5).

To define the limits of the assay, the measurement limits were determined using the limit of blank method (see SI).<sup>[11]</sup> The limit of detection was estimated to 4  $\mu\text{M}$ , while the limit of quantification lies at about 6  $\mu\text{M}$  with a precision of above 90% (see SI Table 1). In conclusion, it is possible to separately quantify MeDAC and BrMeDAC, sharing similar spectroscopical properties, in the same solution. Using this calculation procedure, the assay system was put to the test to determine kinetic parameters of enzymes.

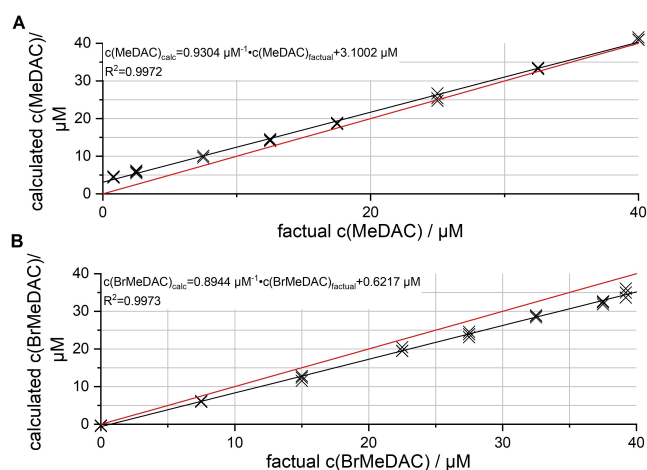


**Figure 5.** Applying correction terms from the line equations of figure 4 to the (new) calculated concentrations of MeDAC (A) and BrMeDAC (B) gave precise and accurate values. The red line represents the ideal case, in which the correlation between calculated and factual concentrations is perfect (slope = 1), the black line represents the measured and calculated concentrations in dependence of the factual ones.

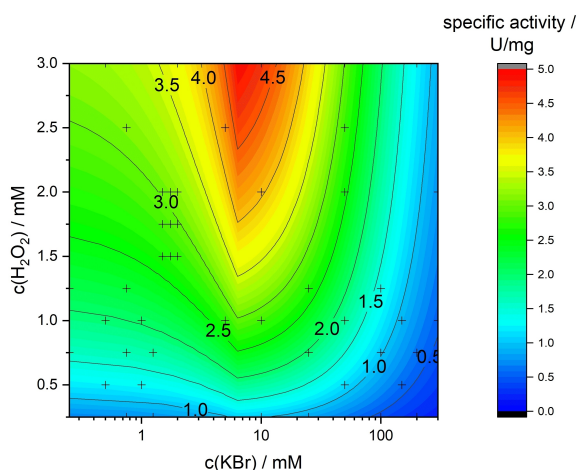


**Figure 6.** Projection of the two-substrate steady state kinetic of the haloperoxidase  $V_{Cl}PO$ . The color code resembles the least-square fit of the kinetic data to the two-substrates substrate excess inhibition-steady-state kinetic according to McMurray, with red areas displaying highest specific activity in the fit. The KBr-ordinate is displayed in logarithmic scale to give an overview on the individual measurements. Residual plots are given in the SI (see SI Figure 10).

## 2.4. Application

To evaluate the MeDAC-assay under conditions where a conversion from MeDAC to BrMeDAC in the presence of oxidizing agents takes place, the kinetic parameters of a halogenating enzyme were determined. For this purpose, the vanadium-dependent chloroperoxidase ( $V_{Cl}PO$ ) from *C. inaequalis* was chosen as it is one of the best characterized haloperoxidases to date.<sup>[12]</sup> HPOs are dependent on two substrates, halide ions and hydrogen peroxide, respectively. To determine unbiased overall Michaelis-constants as well as maximal velocities, kinetics of a two-substrate enzymatic reaction were applied. Therefore, fluorescence intensities with varying concentrations of potassium bromide and hydrogen peroxide were measured with a fixed concentration of MeDAC (30  $\mu\text{M}$ ) and recombinantly produced  $V_{Cl}PO$  (0.3  $\text{ng}\mu\text{L}^{-1}$ ). Due to a proposed inhibition of haloperoxidases by halide ions, the Michaelis-Menten equation was expanded with a substrate-excess-inhibition term according to McMurray<sup>[13]</sup> for both substrates and used as a fit function in OriginPro 2018.<sup>[14]</sup> The kinetic data could be fitted with an  $R^2$  of 0.88 (eq. 4, see Figure 6)

$$v_0 = \frac{v_{\max}}{\left(1 + \frac{K_M(KBr)}{c(KBr)} + \frac{c(KBr)}{K_I(KBr)}\right) \cdot \left(1 + \frac{K_M(H_2O_2)}{c(H_2O_2)} + \frac{c(H_2O_2)}{K_I(H_2O_2)}\right)} \quad (4)$$

with  $v_0$  initial velocity,  $v_{\max}$  maximal velocity,  $K_M$  Michaelis-constant,  $K_I$  inhibitory constant, and  $c$  concentration

Inhibition was visible at higher concentrations for potassium bromide ( $K_I = 56 \pm 7 \text{ mM}$ ) but not for hydrogen peroxide. The  $K_I$  was fitted to be 2E22  $\text{mM}$ , thus, there is no detectable substrate inhibition and the kinetic resembles a generic Michaelis-Menten-kinetic in this direction. For the potassium bromide, the inhibition is below the usual concentration of halide used in other haloperoxidase assays of 100–200  $\text{mM}$ .<sup>[5b]</sup> The Michaelis-constant of 0.19  $\text{mM}$  for (potassium) bromide lies in a similar range compared to previously determined values. For hydrogen peroxide, the values are apart by three orders of magnitude (1.48  $\text{mM}$  and  $< 5 \mu\text{M}$ ) which might be an effect of different pH-values.

The turnover number  $k_{\text{cat}}$  of the enzyme at a concentration of 10  $\text{mM}$  of hydrogen peroxide and 10  $\text{mM}$  of bromide is comparable to results published by other groups for hydrogen peroxide and bromide separately. A side-by-side comparison of kinetic parameters still proves difficult; as the kinetic parameters in literature are either determined at different pH values or the values of the fixed concentration of substrates used are not stated in detail; thus it is not possible to calculate comparable values. In addition, the parameters determined in this work represent global values for  $K_M$  and  $v_{\max}$ , whereas values found in previous studies were determined with a fixed concentration of one substrate while altering the other and *vice versa*, making these values apparent ones. This is also the case for the turnover number  $k_{\text{cat}}$ , which has been calculated using a combination of concentrations for hydrogen peroxide and bromide found in literature. In conclusion, the strong inhibition of  $V_{Cl}PO$  by potassium bromide, already described in related work, could be unfolded and quantified using the MeDAC-

assay.<sup>[5b]</sup> Additionally, the kinetic data that could be deduced for this assay, was mostly in accordance to published data.<sup>[5b]</sup>

It is notable, that during single measurements of the reaction velocity, fluorescence dropped for both, MeDAC and BrMeDAC after 5 minutes, depending on the concentrations of potassium bromide and hydrogen peroxide used (see SI Figures 11 & 12). MeDAC is preferably halogenated in its 3-position. However, other sites can subsequently be halogenated. That may be the reason why the BrMeDAC concentration drops. For kinetic studies this is irrelevant, since the read-out is never used until this late stage for the calculation of the initial velocity ( $v_0$ ).

To finally validate the measured concentrations, samples of  $V_GPO$  with optimal concentrations of hydrogen peroxide (3 mM) and potassium bromide (5 mM) were measured on a HPLC system by extracting the contents with ethyl acetate after defined time periods (120, 300 and 600 s). The peaks observed in the HPLC chromatograms were assigned to MeDAC and BrMeDAC, respectively.

As the chromatograms reveal, there is a significant amount of side-product formed after 10 min, which is negligible after 5 min of reaction time (see SI Figure 13). As the conditions used for this experiment were optimized for a maximum velocity of the enzyme, the effect of the observed side-products may differ for other setups. During the first two minutes of the kinetic measurement the formation of the proposed BrMeDAC from MeDAC could be observed.

### 3. Conclusions

Providing a direct assay for the determination of enzyme kinetics is dependent on the reaction analyzed and often difficult to monitor if starting material and product of the reaction have similar properties. With the assay system presented in this work, following on the bromination of MeDAC to BrMeDAC, we describe a procedure to simultaneously measure starting material consumption and product formation based on a fluorescence readout, neglecting interferences usually suffered for fluorometric measurements (quenching, fluorescence intensity overlaps). With low limits of detection (4  $\mu\text{M}$ ) and quantification (6  $\mu\text{M}$ ), the system provided is sufficiently sensitive to determine enzymatic activity even in low concentrated samples (0.3  $\text{ng } \mu\text{L}^{-1}$  enzyme).

From an economical point of view, the cost of MeDAC lies at around 8 € per gram and can be obtained at various manufacturers like Sigma-Aldrich and Alfa Aesar.<sup>[15]</sup> In contrast, for the broadly used dimedone assay the cost for the monochlorinated compound lies at 310 € per gram, while the monobrominated compound is sold for 2600 € per gram.<sup>[16]</sup> Dimedone itself is cheaper (0.88 € per g) but does not allow a proper quantification as one molecule may be halogenated twice and prevents a correct determination of activity.<sup>[17]</sup> For the dimedone assay, the plethora of side-reactions have also to be accounted for to obtain reliable results.<sup>[6a]</sup> Nevertheless, the dimedone assay appears easier to perform compared to this system: it does not require a complex calibration and is not as

sensitive to additives and changes in pH or molarity. However, many technical difficulties of the MeDAC assay could be overcome applying a normalization and inherent difficulties such as quenching effects could be handled using a calibration, reducing its complexity. All in all the method is mathematically less demanding than alternative approaches e.g. singular value decomposition. The supplemental material provides detailed equations for the reproduction in other labs. To use our system, it would be required to measure the fluorescence intensities of MeDAC and BrMeDAC at their highest concentrations (i.e. 40  $\mu\text{M}$ ) with the given experimental setup and normalize other intensities to this value (i.e. at 450 nm emission normalize to the intensity of 40  $\mu\text{M}$  MeDAC, at 550 nm to the intensity of 40  $\mu\text{M}$  BrMeDAC). In that case, the equations, formulae and functions could simply be adapted without further calibrations. To facilitate the procedure, we provided a Microsoft Excel sheet with the equations found in the supporting information which may be used to calculate concentrations from normalized fluorescence intensities with our buffer system. One has to bear in mind, however, that side-products are formed as shown in the HPLC chromatograms which might hinder a proper read-out if the velocity of the enzyme is too high or the reaction is carried out for too long. The low volume used may be prone to pipetting errors, but an adaptation to quartz cuvettes for fluorescence photometers should yield the same results. Until now, the synthesis of the chlorinated analogue has proven difficult, as several side products are formed and separation of these still proves challenging. As the spectra of MeDAC and BrMeDAC are already quite similar, there might not be a sufficient shift in fluorescence for the chlorinated MeDAC to apply our methodology there, as well. Preliminary results with MeDAC in presence of  $V_GPO$  and chlorine ions have shown a fluorescence intensity decrease for MeDAC (425 nm excitation, 450 nm emission), but no change in fluorescence at the wavelength of BrMeDAC (425 nm excitation, 550 nm emission) during the course of the reaction. Chlorinating activity does seem to be measurable by monitoring MeDAC consumption but without product measurable the calculation would relapse to a simple linear calibration missing intel on fluorescence interactions between both compounds. These observations seem to align with our hypothesis, however further investigation is required in the future.

For kinetic studies, the MeDAC-assay has been shown to yield reliable and reproducible results for reasonable kinetic parameters. To our knowledge, this was the first two-dimensional kinetic investigation on vanadium-dependent haloperoxidases. The kinetic data, especially the  $K_i$ -value towards potassium bromide, supports the proposed substrate-excess inhibition hypothesis for HPOs of *Wever et al.* and *Butler et al.*<sup>[5b,10]</sup> While the direct comparison of kinetic parameters on this enzyme proved difficult as many experimental parameters (and thereby values) differ between publications, the Michaelis-constant for bromide (0.19 mM) as well as the catalytic turnover number (7  $\text{s}^{-1}$  with fixed concentration 10 mM of hydrogen peroxide and 8.5  $\text{s}^{-1}$  with 10 mM potassium bromide) fit in with some of the published data (see Table 1).<sup>[5b]</sup> Especially the  $K_m$ -value for hydrogen peroxide shows a low fit with parameters

determined elsewhere, likely due to the different pH-values utilized. Using this assay, one complete data set of kinetic parameters at the given conditions could be acquired. The presented kinetic data form a coherent data set taking all enzymatic kinetic parameters and their relations to each other into account. These resulting parameters determined with the MeDAC-assay may help increase the overall performance of this enzyme and other homologues in the future.

## Experimental Section

### Synthesis of 3-Bromo-4-Methyl-7-Diethylamino-Coumarin (5b)

The synthesis of the reference compound **5b**, 3-bromo-4-methyl-7-diethylaminocoumarin, was performed according to *Gordeeva et al.*<sup>[9]</sup> To a solution of 0.86 mmol (204 mg) of 7-diethylamino-4-methylcoumarin (**4**) dissolved in 50 mL acetonitrile, 1.06 equivalents (0.92 mmol, 174 mg) of *N*-bromo-succinimide dissolved in 20 mL acetonitrile was added under stirring drop-wisely over 60 min at 25 °C. The solvent was evaporated to dryness and purified on a silica column using toluene-acetone as solvents in a ratio of 40:1. Fractions containing a single spot on a TLC were pooled, evaporated to dryness and analyzed via NMR (see SI Figure 1). The product was obtained in 97% (258 mg, 0.83 mmol) yield.

### Fluorescence Measurements

Fluorescence measurements were performed using a TECAN Infinite M1000 Pro Plate Reader. Greiner 96-well black flat bottom chimney plates were used with a working volume of 250  $\mu$ L. The 2D excitation-emission spectra were measured ranging from excitation wavelengths of 300 nm to 850 nm and emission wavelengths of 320 nm to 850 nm using a wavelength step-size of 2 nm for both. The intensity was measured with a gain of 100 and 25 flashes with a flash frequency of 400 Hz, 20  $\mu$ s integration time, 0  $\mu$ s lag time and 0 ms settle time with excitation and emission bandwidths of 5 nm. The single-point and kinetic measurements were performed using the excitation wavelength of 425 nm and an emission wavelength of 450 nm for the preferential detection of MeDAC and 550 nm for BrMeDAC, as the fluorescence intensities were at least three-fold higher for the targeted compound respectively. The intensity was measured with a gain of 100 and 10 flashes with a flash frequency of 400 Hz, 20  $\mu$ s integration time, 0  $\mu$ s lag time and 0 ms settle time with excitation and emission bandwidths of 5 nm.

### Calculations and Fitting

For the fitting of the 3D-calibrations for both emission wavelengths, the 'Poly-2D'-fit function in OriginPro 2018 was used ( $z = z_0 + a \cdot x + b \cdot y + c \cdot x^2 + d \cdot y^2 + f \cdot x \cdot y$ ). The resulting equation systems were solved for the concentration of MeDAC –still in dependence of *c* (BrMeDAC)- using the analysis tool of GeoGebra (<https://www.geogebra.org/>). The four solutions were solved numerically for concentrations of BrMeDAC using the 'target goal' function in Microsoft Excel (2016) providing a simplex algorithm. Two of the four equations will predict the very same measured fluorescence intensities for a pair of *c*(BrMeDAC) and *c*(MeDAC), thus the difference should be zero. For this condition a BrMeDAC concentration was solved numerically. The normalization for the relative intensities was the measured intensity at the given conditions of MeDAC and BrMeDAC at a concentration of 40  $\mu$ M. For detailed information on the mathematical background and the solution of

the equations, see the corresponding section in the supporting information.

For enzyme kinetics, a two-dimensional Michaelis-Menten fit was combined with the substrate-inhibition term by McMurray as a fit function in OriginPro 2018 (*vide supra*). To predefined concentrations of potassium bromide and hydrogen peroxide in 100 mM Bis-TRIS buffer pH 6, a solution of 30  $\mu$ M MeDAC in 100 mM Bis-TRIS buffer pH 6, 0.3% (v/v) DMSO with 0.3  $\mu$ g mL<sup>-1</sup> recombinantly produced and His-Tag isolated V<sub>C</sub>PO from *C. inaequalis* (see SI Figure 9) at 25 °C was added up to a total volume of 250  $\mu$ L per well to start the reaction. The kinetic was measured for 10 min. The measured intensities were normalized, converted to concentrations, corrected with the corresponding term (see Figure 5) and then plotted against the time. Of each curve obtained, the linear part was then used to determine the slope, which is equivalent to the velocity of the enzyme, and then divided through the enzyme concentration used to obtain the specific enzyme activity. These values were then plotted against the concentration of potassium bromide and hydrogen peroxide and fitted with the 2D-Michaelis-Menten-McMurray function.

### HPLC Measurements

HPLC measurements were carried out at 25 °C using a Lux Amylose-1 column (250\*4.6 mm, Fa. Phenomex) with *n*-heptane:isopropanol in a ratio of 60:40 at a flow rate of 0.5 mL min<sup>-1</sup>. Samples of MeDAC and BrMeDAC, dissolved in *n*-heptane:isopropanol 50:50, were detected at 370 nm with an injection volume of 5  $\mu$ L. The retention time of MeDAC was 9.3 min, the time of BrMeDAC was 10.7 min.

The enzymatic reactions were carried out at 25 °C in 15 mL tubes with 30  $\mu$ M of MeDAC, 3 mM of H<sub>2</sub>O<sub>2</sub> and 5 mM of KBr analogous to the kinetic measurements to ensure comparability between measurements. The tubes were incubated at 800 rpm in a HLC tube shaker (Citabis) and one sample each extracted three times with 15 mL ethyl acetate after 120, 300 or 600 s. The extract was evaporated to a small volume of ca. 1 mL, transferred into an Eppendorf tube and evaporated to dryness. Finally, the sample was dissolved in 150  $\mu$ L *n*-heptane:isopropanol 50:50 and measured by HPLC-analysis.

## Acknowledgements

The authors thank the Forschungszentrum Jülich GmbH and the Heinrich-Heine University Düsseldorf for their support. The work was supported by grants from the Deutsche Forschungsgemeinschaft (GRK2158), the Bioeconomy Science Center, and the European Regional Development Fund (ERDF: 34.EFRE 0300096 and 34.EFRE 0300097) within the project CLIB-Kompetenzzentrum Biotechnologie CKB). The scientific activities of the Bioeconomy Science Center were financially supported by the Ministry of Innovation, Science and Research of the German federal state of North Rhine-Westphalia MIWF within the framework of the NRW Strategieprojekt BioSC (No. 313/323-400-00213). The scientific activities of the Bioeconomy Science Center were financially supported by the Ministry of Innovation, Science and Research of the German federal state of North Rhine-Westphalia MIWF within the framework of the NRW Strategieprojekt BioSC (No. 313/323-400-00213). Moreover, we are grateful to Nora Bitzenhofer, Jan Gebauer, Marvin Mantel, Pascal Schneider and Birgit Henßen for

the fruitful discussions and especially the two latter for the analytical support.

### Conflict of Interest

The authors declare no conflict of interest.

**Keywords:** halogenation · fluorescence spectroscopy · kinetics · enzyme catalysis · hypobromite

- [1] C. M. Harris, R. Kannan, H. Kopecka, T. M. Harris, *J. Am. Chem. Soc.* **1985**, *107*, 6652–6658.
- [2] T. Fasina, F. Ejjah, N. Idika, C. Dueke-eze, *Int. J. Biol. Chem.* **2013**, *7*, 79–85.
- [3] C. Torborg, M. Beller, *Adv. Synth. Catal.* **2009**, *351*, 3027–3043.
- [4] a) F. Ausfelder, *Flexibilitätsoptionen in Der Grundstoffindustrie: Methodik, Potenziale, Hemmnisse: Bericht Des Ap V. 6“ Flexibilitätsoptionen Und Perspektiven in Der Grundstoffindustrie“ Im Kopernikus-Projekt“ Synergie-Synchronisierte Und Erngieadaptive Produktionstechnik Zur Flexiblen Ausrichtung Von Industrieprozessen Auf Eine Fluktuierende Energieversorgung*, DECHEMA Gesellschaft für Chemische Technik und Biotechnologie eV, **2018**; b) Euro Chlor, a Sector Group of Cefic, **2018**.
- [5] a) D. R. Morris, L. P. Hager, *J. Biol. Chem.* **1966**, *241*, 1763–1768; b) R. Wever, B. E. Krenn, R. Renirie, *Methods Enzymol.* **2018**, *605*, 141–201.
- [6] a) H. China, Y. Okada, T. Dohi, *Asian J. Org. Chem.* **2015**, *4*, 1065–1074; b) C. Wagner, I. M. Molitor, G. M. König, *Phytochemistry* **2008**, *69*, 323–332.
- [7] a) S. M. K. McKinnie, Z. D. Miles, B. S. Moore, *Methods Enzymol.* **2018**, *604*, 405–424; b) N. Tanaka, Z. Hasan, R. Wever, *Inorg. Chim. Acta* **2003**, *356*, 288–296.
- [8] K. Starzak, A. Matwijczuk, B. Creaven, A. Matwijczuk, S. Wybraniec, D. Karcz, *Int. J. Mol. Sci.* **2019**, *20*, 281.
- [9] N. A. Gordeeva, M. A. Kirpichnok, N. S. Patalakha, I. I. Grandberg, *Chem. Heterocycl. Compd.* **1990**, *26*, 1329–1337.
- [10] a) R. R. Everett, H. S. Soedjak, A. Butler, *J. Biol. Chem.* **1990**, *265*, 15671–15679; b) A. Butler, *Coord. Chem. Rev.* **1999**, *187*, 17–35.
- [11] a) D. A. Armbruster, T. Pry, *Clin. Biochem. Rev.* **2008**, *29 Suppl 1*, S49–52; b) A. Shrivastava, V. Gupta, *Chron. Young Sci.* **2011**, *2*, 21–25.
- [12] a) W. Hemrika, R. Renirie, S. Macedo-Ribeiro, A. Messerschmidt, R. Wever, *J. Biol. Chem.* **1999**, *274*, 23820–23827; b) Z. Hasan, R. Renirie, R. Kerkman, H. J. Ruijssenaars, A. F. Hartog, R. Wever, *J. Biol. Chem.* **2006**, *281*, 9738–9744; c) J. J. Dong, E. Fernandez-Fueyo, J. Li, Z. Guo, R. Renirie, R. Wever, F. Hollmann, *Chem. Commun. (Camb.)* **2017**, *53*, 6207–6210; d) J. W. Van Schijndel, P. Barnett, J. Roelse, E. G. Vollenbroek, R. Wever, *Eur. J. Biochem.* **1994**, *225*, 151–157; e) E. Fernández-Fueyo, M. van Wingerden, R. Renirie, R. Wever, Y. Ni, D. Holtmann, F. Hollmann, *ChemCatChem* **2015**, *7*, 4035–4038.
- [13] D. R. P. Murray, *Biochem. J.* **1930**, *24*, 1890–1896.
- [14] E. de Boer, R. Wever, *J. Biol. Chem.* **1988**, *263*, 12326–12332.
- [15] Sigma-Aldrich, **2020**, <https://www.sigmaaldrich.com/catalog/product/aldrich/d87759?lang=de&region=DE>, date of access: 05.03.2020 .
- [16] a) Sigma-Aldrich, **2020**, <https://www.sigmaaldrich.com/catalog/product/aldrich/s812110?lang=de&region=DE>, date of access: 05.03.2020; b) Alfa Aesar, **2020**, <https://www.alfa.com/de/catalog/H51035/>, date of access: 05.03.2020.
- [17] Alfa Aesar, **2020**, <https://www.alfa.com/de/catalog/A10140/>, date of access: 05.03.2020 .

Manuscript received: June 18, 2020  
Revised manuscript received: August 17, 2020